35-fold when measured immediately following the return to normal pH solution. This effect is only partially reversible. Fig. 2 shows K currents recorded in pH 7.4 solution before and 2 min after a 7.5 min. exposure to pH 11. The closing of K channels remains slowed by the high-pH treatment. As with TNBS treatment, high pH seems to have its greatest effects on the closing rates of K channels. Activation rates are less affected by the procedure. The effects of high-pH treatment are larger and less reversible following long exposures. Following short exposure (<2 min), the K-channel closing kinetics return towards control on a time course of minutes. Like TNBS, high-pH treatment increases the resistance of K channels to block by 4AP. Fig. 3 shows the time course of block by 4AP in a fiber pretreated with pH-11.5 solution. Only 40% of the slow component of the tail current was blocked after 280 s. Since this fiber showed no slow component in the tail current before treatment with high pH, this result indicates that high-pH treatment induced 4AP resistance along with the kinetic changes.

These data suggest that 4AP normally blocks K channels by binding to a site accessible to modification by external TNBS and high pH. Since both of these agents have dramatic effects on the kinetics of K channel closing, and since the K channels that close slowly in untreated fibers are also resistant to 4AP, it seems possible that 4AP binds to a site involved in K-channel gating. Our results also raise the possibility that the various subpopulations of K channels in myelinated nerve fibers may be interconvertable. Fink and Wettwer (1978) have shown that exhaustion in skeletal muscle fibers changes the properties of the K conductance, converting the channels to a permanently open state that is more resistant to block by 4AP. The characteristics of K channels in myelinated nerve fibers may be regulated by similar mechanisms.

Received for publication 4 May 1983.

REFERENCES

Cahalan, M. D., and P. A. Pappone. 1983. Chemical modification of potassium channel gating in frog myelinated nerve by trinitrobenzene sulphonic acid. *J. Physiol. (Lond.)*. In press.

Dubois, J. M. 1981. Evidence for the existence of three types of potassium channels in the frog Ranvier node membrane. *J. Physiol. (Lond.)*. 318:297–316.

Fink, R., and E. Wettwer. 1978. Modified K-channel gating by exhaustion and the block by internally applied TEA and 4-aminopyridine in muscle. *Pflügers Arch. Eur J. Physiol.* 374:289–292.

Ulbricht, W., and H.-H. Wagner. 1976. Block of potassium channels of the nodal membrane by 4-aminopyridine and its partial removal on depolarization. *Pflügers Arch. Eur J. Physiol.* 367:77–87.

CELL-TO-CELL CHANNELS WITH TWO INDEPENDENT GATES IN SERIES, REGULATED BY MEMBRANE POTENTIALS, BY pCa_i AND BY pH_i

B. Rose, S. J. Socolar and A. L. Obaid

Department of Physiology and Biophysics, University of Miami School of Medicine, Miami, Florida 33101

Junctional conductance (g_j) between cells in *Chironomus* salivary glands is modulated by membrane potentials, $[Ca^{2+}]_i$, and pH_i. In the studies we describe here, the conductance variation appears to arise from two gates in series in each cell-to-cell channel; we show that each such gate responds to all three modulators (1).

We studied g_j in cell pairs, using two independent voltage clamps to set the potentials of the cells and to measure g_j. We found (Fig. 1 *A Inset*) that when $E_1 = E_2 = E$, steady state g_j varies sigmoidally between an upper asymptote ($g_j$max) and zero.

When g_j is examined as a function of E_j ($E_j = E_1 - E_2$, in Fig. 2), it becomes evident that g_j varies widely at any given E_j, is not symmetric about $E_j = 0$ (this does not imply a rectifier), but depends on E_1 and E_2. Hence E_j plays little or no role in determining g_j. The curves suggest that the fixed potential imposes an upper limit on g_j however negative the other potential. This is expected if g_j is the product of an E_1-dominated function and an E_2-dominated function, both sigmoid.

This pattern of g_j dependence on membrane potentials suggests that each cell-to-cell channel has two voltage-sensitive gates in series, pertaining to the two cell membranes of the junction. We postulate that the steady state g_j is the resultant of two simultaneous but independent voltage sensitive open/closed equilibria, one within each population of gates (i.e., one on each side of the junction), with open gates occurring on each side with a probability $\{1 + \exp[A(E_k - E_0)]\}^{-1}$, where A and E_0 are constants and E_k is the potential of the respective side. This model fits well the data of experiments such as that of Fig. 1, where $E_1 = E_2$. Although the model takes no account of E_j, it fits the g_j data for $E = -E_2$ despite presence of substantial E_j values (Table I). This is expected if the potential determining the state of a given gate is the corresponding perichannel membrane potential (E_p)—the potential

Biophys. J. © Biophysical Society · 0006-3495/84/01/064/03 $1.00
Volume 45 January 1984 64–66

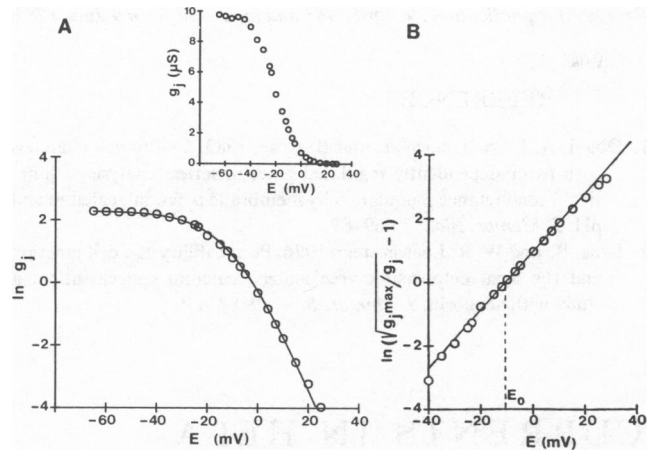

FIGURE 1 Dependence of junctional conductance g_j on membrane potentials E. *A*, Plot of ln g_j vs. E ($=E_1 = E_2$). *Inset*: plot of g_j vs. E. *B*, Plot of $\ln[g_j\max/g_j)^{1/2} - 1]$ vs. E; according to the two-gate model, $\ln[g_j\max/g_j)^{1/2} - 1] = A(E - E_0)$. We took $g_j\max = 9.8$ μS. The solid line (——) in *A* was calculated with this $g_j\max$, the slope ($A = 0.093$ mV^{-1}) of the straight-line-fit to the circles (○) (correlation coefficient $r = 0.998$), and $E_0 = -10$ mV.

across the small element of cell membrane in which that gate's end of the channel is embedded. The fit is absent when $E_1 \neq \pm E_2$.

E_p for a given gate differs from the cellular E only to the extent that the potential in the intercellular gap, at the

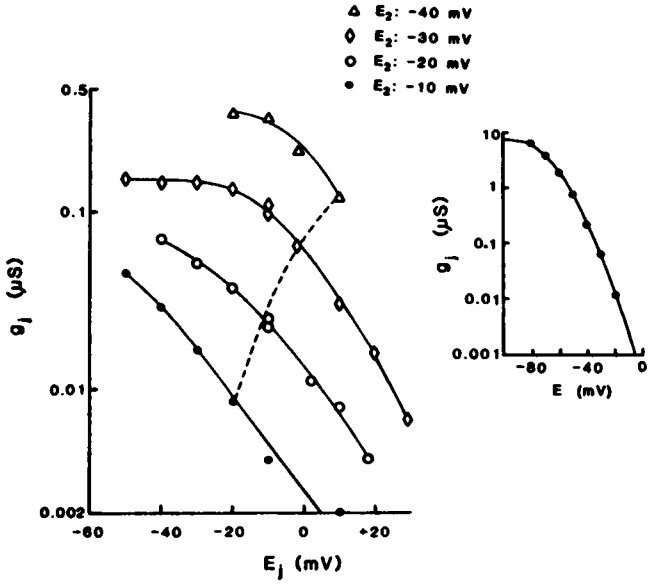

FIGURE 2 Dependence of g_j on E_1 and E_2 ($E_1 \neq E_2$): is E_j the determinant? With E_2 clamped at a single value, g_j was measured for various values of E_1. This was done for different E_2; results are plotted against E_j ($E_1 - E_2$). Solid lines (——) connect points with equal E_2. Dashed line (---) is drawn through points with $E_1 = -30$ mV, to show that the data imply a set of curves (i.e., with E_1 constant) that approximate mirror images of the solid curves across the line $E_j = 0$. *Inset*: plot of g_j vs. E ($E_1 = E_2$) for the same junction. Reproduced with permission from *J. Membr. Biol.*

TABLE I
JUNCTIONAL CONDUCTANCE IN THE PRESENCE OF TRANSJUNCTION POTENTIAL

E_1 (mV)	E_2 (mV)	E_j (mV)	Observed g_j (μS)	Calculated g_j (μS)
−28	+30	58	0.138	0.133
−19	+20	39	0.179	0.185
−10	+12	22	0.155	0.200
+13	−25	38	0.132	0.395
−10	+5.5	15.5	0.194	0.313

All measurements are on the same cell pair. Values in the last column were calculated from $g_j = 19\{1 + \exp[0.073(E_1 + 28.2)]\}^{-1}\{1 + \exp[0.073(E_2 + 28.2)]\}^{-1}$, where the parameters in the equation were derived by analysis of $g_j(E)$ for 16 data points with $E_1 = E_2$ (correlation coefficient $r = 0.992$).

level of the given channel, differs from that in the bulk extracellular medium. An amusing point is that if the gap region is taken to be isolated from the bulk medium by a high-resistance barrier (e.g., a *zonula occludens*), the calculated $|E_p|$ approaches the limit $1/2|E_1 - E_2|$, E_p then having opposite signs for the two channel gates. Hence in

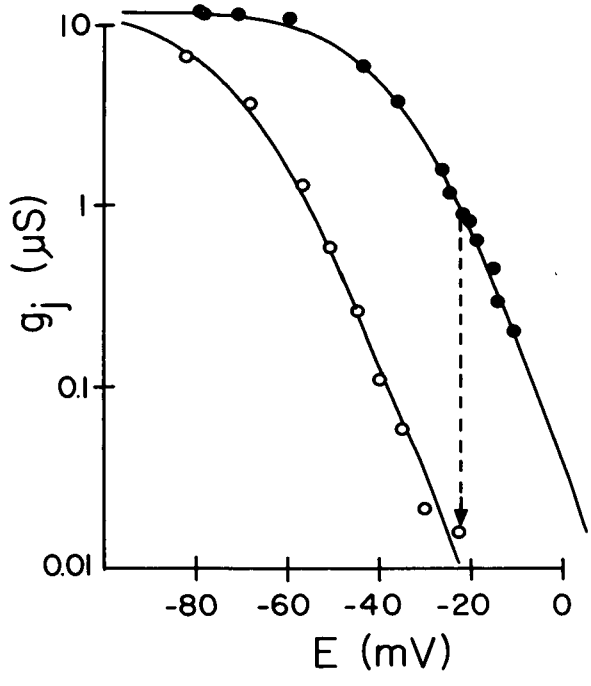

FIGURE 3 Effect of decrease in pCa_i on the g_j vs. E relation. A cell pair's g_j vs. E relation was determined in control condition (•). The cells were then superfused with medium containing 5 mM NaCN, which lowers pCa_i (2). After g_j (at −24 mV) had stabilized at 0.02 μS, the data depicted by open circles (○) were measured. Both sets of data were analyzed according to the two-gate model, with $g_j\max = 12$ μS providing best fit: r(control) = 0.995; r(CN) = 0.997. The solid lines (——) represent calculated g_j, with $g_j\max$ and the other parameters derived from the analysis. *Control*: $A = 0.085$ mV^{-1}, $E_0 = -33.5$ mV; CN$^-$: $A = 0.078$ mV^{-1}, $E_0 = -67.5$ mV. Reproduced with permission from *J. Membr. Biol.*

this case channel gates controlled by E_p would look as if controlled by E_j.

When pCa_i or pH_i is altered, the effect is to shift the $g_j(E)$ curve along the E axis without other changes (see e.g., Fig. 3). From this finding we conclude that E, Ca^{2+}, and H^+ all affect the same gates—although we do not know whether any of these acts directly on the gates—and that Ca^{2+} and H^+ do so without influencing the voltage sensitivity (A) of the gates.

Received for publication 29 April 1983 and in revised form 9 June 1983.

REFERENCES

1. Obaid, A. L., S. J. Socolar, and B. Rose. 1983. Cell-to-cell channels with two independently regulated gates in series: analysis of junctional conductance modulation by membrane potential, calcium and pH. *J. Membr. Biol.* 73:69–89.
2. Rose, B., and W. R. Loewenstein. 1976. Permeability of a cell junction and the local cytoplasmic free ionized calcium concentration: a study with aequorin. *J. Membr. Biol.* 28:87–119.

SINGLE Ca^{++} DEPENDENT K^+ CURRENTS IN HELA CANCER CELLS

R. Sauvé, G. Bedfer, and G. Roy
Départements de physiologie et de physique, Université de Montréal, Montréal, Québec, H3C 3J7, Canada

Using the extracellular patch-clamp method (1), we have investigated the single-channel events underlying the electrophysiological properties of HeLa cells, a human cell line obtained from an epidermoid carcinoma of the cervix. In a first paper, we presented recordings of discrete current jumps observed with patch electrodes containing solely KCl (75 mM up to 300 mM)(2). This particular channel was found to be mainly permeable to K^+ and showed multiple levels of conductance (40 pS and 28 pS). In addition, the channel I-V curves obtained at various KCl concentrations in the patch electrode were all characterized by a strong inward-rectification effect. We present in this paper recordings of another type of single channel event, made during cell-attached and outside-out patch-clamp experiments. In the cell-attached configuration using electrodes filled with normal saline (140 NaCl + 5 KCl), we detected clear outward-current jumps occurring mainly in bursts. We also found, through various outside-out patch clamp experiments, that this particular channel was mainly permeable to potassium ion and showed Ca^{++}-dependent open-closed kinetics.

MATERIALS AND METHODS

HeLa cells were obtained from the Institut Armand-Frappier in Montreal and subcultured in Falcon bottles (75 cm^2, #3024). The culture medium was MEM, Earle base (Gibco #F-11, Gibco Diagnostics, Chagrin Falls, OH) with 25 mM HEPES buffer and 6 mM bicarbonate. This medium was supplemented with 10% fetal calf serum (Gibco #G14H1) and 1 μg/ml of gentamycine. The cells were grown in monolayers in plastic petri dishes, and used for patch experiments two or three days after being subcultured.

Unless specified otherwise all cell-attached patch-clamp experiments reported in this work were carried out with patch electrodes containing 140 mM NaCl, 5 mM KCl, 5 mM $CaCl_2$, 0.81 Mg SO_4 and 10 HEPES buffered at pH 7.2. We will refer to this solution as "Earle-modified." For outside-out patch-clamp experiments, we used pipettes filled with a solution containing 150 mM KCl, 3 mM HEPES (pH 7.2), to which various concentrations of $CaCl_2$ were added (0.1–2 mM). In both types of experiments, the external medium was an Earle-HEPES solution with 116 mM NaCl, 5.4 mM KCl, 1.8 mM $CaCl_2$, 0.81 $MgSO_4$, 6 $NaHCO_3$, 1 NaH_2PO_4, 5.5 glucose and 25 HEPES (pH 7.3). All experiments were done at room temperature (23°C). The essentials of our setup have been described in detail elsewhere (2). Each experiment was usually recorded on FM tape at a bandwidth of 1 KHz (H.P. 3964A) before being low-pass filtered (4 pole-Bessel) and digitized for computer analysis (MINC 11/23, Digital Equipment Corp., Marlboro, MA). The current jump amplitudes were derived from current amplitude histograms. The time intervals between opening or closing events were detected by setting, for a selected portion of the time record, an intermediate reference level corresponding to the current value with the lowest probability of occurrence. Open and closed time intervals were thus taken as the time the signal remained above or below this reference current level, following the detection of two transitions of opposite polarity.

RESULTS

Fig. 1 *A–E* shows single-channel recordings obtained on two different HeLa cells in cell-attached patch-clamp experiments carried out with patch electrodes filled with normal saline. Outward current-jumps due mainly to potassium ions can readily be observed. The single-channel conductance at low membrane potentials was estimated at 10 pS. Two basic fluctuations patterns are presented. With certain cells (Fig. 1 *A* and *B*), the recorded single-channel events appeared mainly as short bursts of channel openings separated by longer silent periods. With other cells we observed a different channel behavior, characterized by longer channel openings frequently interrupted by brief transitions towards a closed state (Fig. 1 *C–E*). In many cases, we found (Fig. 1 *D*) a random mixture of these two basic fluctuation patterns. A time-interval histogram analysis of these particular records, an example of which is given in Fig. 2 *A* and *B* for the time record shown in Fig. 1 *D*, indicates that at least three closed states and probably two open states are present. In fact, two of the estimated

BIOPHYS. J. © Biophysical Society · 0006–3495/84/01/066/03 $1.00
Volume 45 January 1984 66–68